




FLCN regulates transferrin receptor 1 transport and iron homeostasis

Received for publication, July 21, 2020, and in revised form, January 19, 2021. Published, Papers in Press, February 17, 2021, <https://doi.org/10.1016/j.jbc.2021.100426>

Xiaojuan Wang[†], Hanjie Wu[†], Lingling Zhao[†], Zeyao Liu, Maozhen Qi, Yaping Jin*, and Wei Liu*

From the College of Veterinary Medicine, Northwest A&F University, Yangling, Shanxi, China

Edited by Phyllis Hanson

Birt–Hogg–Dubé (BHD) syndrome is a multiorgan disorder caused by inactivation of the folliculin (FLCN) protein. Previously, we identified FLCN as a binding protein of Rab11A, a key regulator of the endocytic recycling pathway. This finding implies that the abnormal localization of specific proteins whose transport requires the FLCN-Rab11A complex may contribute to BHD. Here, we used human kidney-derived HEK293 cells as a model, and we report that FLCN promotes the binding of Rab11A with transferrin receptor 1 (TfR1), which is required for iron uptake through continuous trafficking between the cell surface and the cytoplasm. Loss of FLCN attenuated the Rab11A–TfR1 interaction, resulting in delayed recycling transport of TfR1. This delay caused an iron deficiency condition that induced hypoxia-inducible factor (HIF) activity, which was reversed by iron supplementation. In a *Drosophila* model of BHD syndrome, we further demonstrated that the phenotype of BHD mutant larvae was substantially rescued by an iron-rich diet. These findings reveal a conserved function of FLCN in iron metabolism and may help to elucidate the mechanisms driving BHD syndrome.

Loss of folliculin (FLCN) has been associated with Birt–Hogg–Dubé (BHD) syndrome, which is characterized by frequent development of skin tumors, lung cysts, and a high risk of kidney cancer. FLCN regulates a wide range of cellular processes, such as amino acid homeostasis, energy metabolism, biogenesis of lysosomes and mitochondria, membrane transport, cytoskeletal remodeling, and primary cilia formation (1). However, the primary cause of BHD is still unknown. This uncertainty is partially due to the observation that both the growth-promoting protein mTOR (2–9) and the energy sensor AMP-activated protein kinase (10–13) can be either activated or suppressed upon FLCN loss. It has thus been speculated that FLCN regulates these two pathways through varied

mechanisms, depending on the specific cellular and tissue contexts.

FLCN is conserved from yeast to humans, implying that it necessarily regulates certain fundamental cellular processes. Consistent with this hypothesis, emerging evidence has revealed important roles of FLCN during vesicular trafficking, which is a highly conserved process in eukaryotic cells. Indeed, before FLCN was initially identified in humans and subsequently linked to BHD, the Kaiser group had identified a group of yeast genes governing the movement of the amino acid permease Gap1p from the Golgi apparatus to the plasma membrane (14). Among these genes are LST7, an ortholog of the mammalian FLCN (15), and LST4, an ortholog of FNIP1/2 (16, 17); the latter has been found to form a complex with FLCN in most (if not all) functions of FLCN (18–21). Both LST7 and LST4 had been believed to be components of specific transport machinery (14), but the precise mechanisms remained unknown. In 2012, a structural study uncovered a differentially expressed in normal cells and neoplasia (DENN) domain in the FLCN C terminus (22). Because some DENN-containing proteins are activators of Rab proteins (Rabs), which are key regulators of vesicular trafficking, FLCN has been suspected to regulate protein transport *via* Rabs (22). Shortly after this discovery, two studies demonstrated that FLCN regulates the intracellular transport of EGFR. In one study (23), FLCN was found to promote the movement of EGFR from early endosomes to the cell surface by acting as a guanine nucleotide exchange factor (GEF) of Rab35; in the other study, FLCN was found to be a GTPase-activating protein (GAP) of Rab7 and to prevent the transport of EGFR from early to late endosomes (24). At almost the same time, our group found that the amino acid permease PAT1 (also called slc36A1) is a cargo protein of FLCN (9). We further demonstrated that FLCN promotes the localization of PAT1 on the plasma membrane and inhibits its localization on lysosomes through the Rab11A-mediated pathway (25). This relocalization of PAT1 helps cells to acquire amino acids from the environment while maintaining a robust lysosomal amino acid pool that stimulates mTOR. This function of FLCN seems to be conserved in yeast (14), fly (26) and human cells (25). Regarding the underlying mechanism, we did not find clear GEF or GAP activity of FLCN toward Rab11A. Instead, we found that FLCN promotes the binding of PAT1 to Rab11A in a dose-dependent manner (25). Through a similar mechanism,

[†] These authors contributed equally to this work.

* For correspondence: Yaping Jin, yapingjin@163.com; Wei Liu, wliu20cn@nwafu.edu.cn.

Present address for Xiaojuan Wang: National Research Center for Veterinary Medicine, Pulike Biological Engineering Inc, Luoyang, Henan 471000, China.

Present address for Lingling Zhao: School of Laboratory Medicine and Life Sciences, Wenzhou Medical University, Wenzhou, Zhejiang 325035, China.

FLCN regulates iron metabolism

FLCN has been found to promote the interaction between Rab34 and its effector, RILP, during the positioning of lysosomes (27). Based on these findings, one appealing hypothesis is that the diversified BHD phenotypes might be due to the abnormal localization of specific FLCN substrates. In the current study, we identified transferrin receptor 1 (TfR1, or CD71) as a new substrate of FLCN and thus linked FLCN to iron metabolism.

Iron is an essential nutrient for many biological processes, such as oxygen delivery and storage, DNA metabolism, and energy production. Both iron deficiency and iron overload can cause pathological changes (28). TfR1 is a ubiquitously expressed membrane protein. Most mammalian cells obtain iron from plasma *via* TfR1. Most Fe³⁺ ions in the plasma are loaded on transferrin (Tf), a ferric iron carrier produced mainly in the liver. The Tf-Fe³⁺ complex (called holo-Tf) binds to TfR1 and then enters the cell through membrane invagination. Once Fe³⁺ is released inside the cell, free Tf-TfR1 is sent back to the cell surface for another round of iron uptake. Blocking the cellular trafficking of TfR1 inhibits iron uptake and causes iron deficiency disorders (29, 30). On the other hand, high iron can be toxic by generating deleterious reactive oxygen species (ROS). Therefore, cells have evolved sophisticated mechanisms to control the iron pool (31). The promoter region of the *TfR1* gene contains a hypoxia response element (HRE). Hypoxia-inducible factor (HIF) family transcription factors bind this HRE and directly activate TfR1 transcription (32). *Via* a feedback mechanism, iron deficiency can stabilize the HIF protein by inactivating prolyl hydroxylases (PHDs), which utilize iron as a cofactor to target HIF for degradation (33). The 3' noncoding region of *TfR1* mRNA forms stem-loop structures called iron-responsive elements (IREs). Iron regulatory proteins (IRP1 and IRP2) bind these IREs and prevent degradation of the mRNA (34). A robust iron pool increases iron-sulfur cluster production. The binding of IPRs with iron-sulfur clusters either converts IRP1 into a functional aconitase, which translocates to mitochondria to catalyze respiratory chain reactions, or directs IRP2 for degradation (35, 36). TfR1 can be regulated at the protein level. The TfR1 protein is constantly degraded in lysosomes (37–39). Depletion of iron by iron chelators such as desferrioxamine (DFO) increases the TfR1 protein level, but the mechanism is not fully understood (40).

Here, we report that FLCN regulates TfR1 transport through the Rab11A-mediated pathway. Loss of FLCN delays the recycling of TfR1 and decreases the iron pool. These findings provide new insights for deciphering the mechanisms underlying BHD syndrome.

Results

FLCN promotes the binding of TfR1 to Rab11A

In a previous study, we carried out coimmunoprecipitation (co-IP) assays and discovered that FLCN promotes the binding of PAT1 to Rab11A (25). To determine whether FLCN specifically regulates PAT1, we also examined TfR1, which is

continuously transported by Rab11A. Surprisingly, we found that FLCN also bound to TfR1, and loss of FLCN decreased the TfR1-Rab11A interaction (Fig. 6D in (25)).

However, these data were obtained in cells with GFP-Rab11A overexpression. To eliminate the potential artifacts caused by GFP-Rab11A, we repeated these assays in normal HEK293 cells using a monoclonal anti-TfR1 antibody for the precipitation experiment. Under steady-state conditions, TfR1 showed little interaction with endogenous Rab11A or FLCN (Fig. 1A), probably because under physiological conditions, only a small amount of TfR1 is transported by Rab11A and FLCN. Then, we decided to induce iron deficiency before the assay, based on the following two considerations. First, low iron levels can increase TfR1 expression (31); thus, co-IP would be easier to perform under these conditions. Second, we speculated that low iron levels may stimulate iron uptake by enhancing the TfR1-Rab11A interaction. To decrease the iron pool, we incubated cells with DFO, which is a clinically used iron chelator (41). We detected both Rab11A and FLCN in the TfR1 precipitates from cells treated with 100 μM DFO for 12 h. Moreover, the amount of TfR1-bound Rab11A was decreased in *FLCN*^{-/-} cells (Fig. 1B). These results demonstrate that FLCN promotes the TfR1-Rab11A interaction, particularly under the iron-deficient conditions.

FLCN has been found to bind to different Rabs *via* its C-terminal DENN domain (23–25, 27). It is thus conceivable that FLCN might bind to TfR1 *via* a region other than its DENN domain. To test this hypothesis, we constructed plasmids expressing different forms of FLCN proteins, including wild-type FLCN (1–579), the N-terminal region (1–340), and the DENN domain (341–579), fused to a C-terminal HA tag. To exclude the influence of endogenous FLCN, we transfected these plasmids into *FLCN*^{-/-} cells. Twenty-four hours after plasmid transfection, the cells were deprived of iron by incubation with 100 μM DFO for 12 h. The cell lysates were precipitated with an anti-HA antibody, followed by western blot (WB) analysis. As anticipated, both FLCN and its N-terminal region bound to TfR1; however, there was only a weak interaction between TfR1 and the FLCN DENN domain (Fig. 1C).

Loss of FLCN delays the recycling transport of TfR1

We used a fluorescence conjugated transferrin (FITC-Tf) to monitor the trafficking of TfR1. Cells were incubated with 20 μg/ml FITC-Tf on ice for 20 min. At low temperatures, Tf still bound to TfR1 on the cell surface, but endocytosis was terminated. After the unbound FITC-Tf was washed away, the cells were transferred to 37 °C to reinitiate endocytosis.

When the cells were transferred to 37 °C for 5 min, we observed similar levels of FITC-Tf in both wild-type and *FLCN*^{-/-} cells. In addition, FITC-Tf translocated to an intracellular location very similar to the perinuclear recycling center (PRC, arrows in Fig. 2A), where Rab11A normally accumulates (42, 43). This finding implies that FLCN has little influence on the translocation of TfR1 from the cell surface into the cell. After membrane trafficking was reinitiated by

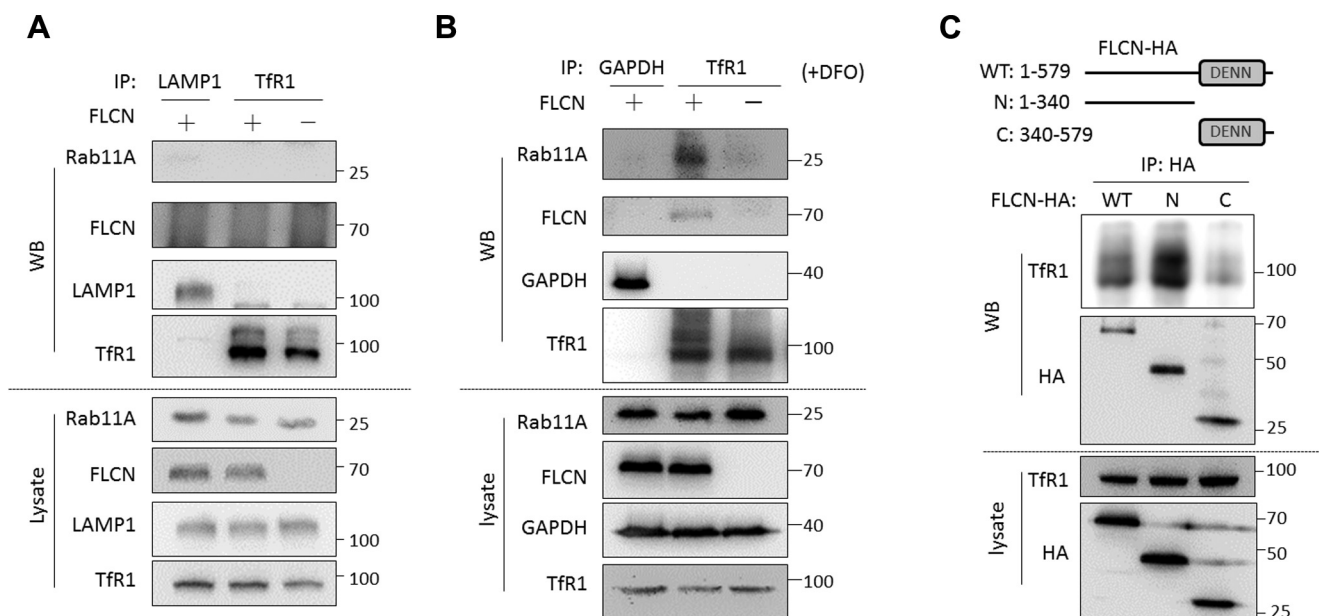


Figure 1. Co-IP assays of the protein-protein interactions. A, cells cultured under normal conditions were lysed. The cell lysates were precipitated with monoclonal antibodies against either LAMP1 (negative control) or TfR1, followed by western blotting with the indicated antibodies. B and C, similar assays as described in A, except that cells were deprived of iron by incubation with 100 μ M DFO for 12 h. In C, plasmids containing different FLCN-HA constructs were transfected into *FLCN*^{-/-} cells to exclude the influence of endogenous FLCN.

incubation at 37 °C for 50 min, the level of FITC-Tf was markedly decreased in wild-type cells (Fig. 2A), but a substantial amount of FITC-Tf was retained in *FLCN*^{-/-} cells (Fig. 2, A and B), suggesting that loss of FLCN delayed the recycling of TfR1.

Uptake of Tf-bound iron is decreased by FLCN loss

To examine the uptake rate of Tf-bound iron, we employed a recently developed method using calcein-AM, a membrane-permeable, fluorescent iron probe whose fluorescence is quenched by binding with iron.

Cells were first stained with 0.4 μ M calcein-AM for 10 min and then incubated with 10 μ g/ml holo-Tf for 3 h. After holo-Tf enters the cells and releases the Tf-bound iron, the intracellular calcein-AM signal decreases. The calcein signal can be measured by flow cytometric analysis, and the reduction in the signal after incubation with holo-Tf (representing the quenched iron pool, QIP) correlates with the amount of holo-Tf taken up by the cells (44). The results revealed that the QIP was decreased in *FLCN*^{-/-} cells, indicating reduced uptake of holo-Tf (Fig. 2C).

Suppression of FLCN decreases the iron pool

We carried out a colorimetric ferrozine-based assay to measure the total cellular iron concentration directly. Compared with wild-type cells, *FLCN*^{-/-} cells exhibited a trend of reduced total iron levels (Fig. 3A), although the difference was not statistically significant ($p = 0.136$, based on three repeated experiments).

We used calcein-AM staining to assess the labile iron pool. *FLCN*^{-/-} cells had stronger calcein signals than wild-type cells,

suggesting that the labile iron pool was decreased by FLCN loss (Fig. 3B). When the iron pool is depleted, the cellular ferritin is degraded to release stored iron. Indeed, the level of FTH, a component of the ferritin protein complex, was decreased in *FLCN*^{-/-} cells (Fig. 3C).

In response to iron deficiency, the expression of iron assimilation genes, including TfR1 and the ferrous iron (Fe²⁺) transporter, also called divalent metal transporter 1 (DMT1, or SLC11A2), increases. These increases can be achieved through multiple mechanisms, including transcriptional activation by HIF (32, 45) and inhibition of mRNA degradation by the IRP-IRE system (34). The mRNA levels of these genes can be used as indicators of the iron status.

We performed real-time PCR (RT-PCR) to measure mRNA levels. A control assay showed that deprivation of iron by DFO chelation increased the expression of both TfR1 and DMT1 (Fig. 3D). Importantly, loss of FLCN produced a similar result but to a lesser extent than DFO treatment, suggesting that FLCN deficiency is less potent than DFO in decreasing the iron pool. Consistent with previous reports that FLCN inhibits the transcriptional coactivator PGC-1 α (12, 13, 46–48), PGC-1 α expression was increased in *FLCN*^{-/-} HEK293 cells. In addition, DFO increased PGC-1 α expression but to a lesser extent than FLCN loss (Fig. 3D), probably indicating that FLCN inhibits PGC-1 α mainly through iron-independent mechanisms. We analyzed two cell lines expressing different short hairpin RNAs (shRNAs) of FLCN (shFLCN) (9) and found that the expression of both TfR1 and DMT1 was increased (Fig. 3E).

We searched the published databases for expression data related to the genes downstream of FLCN. Interestingly, we

FLCN regulates iron metabolism

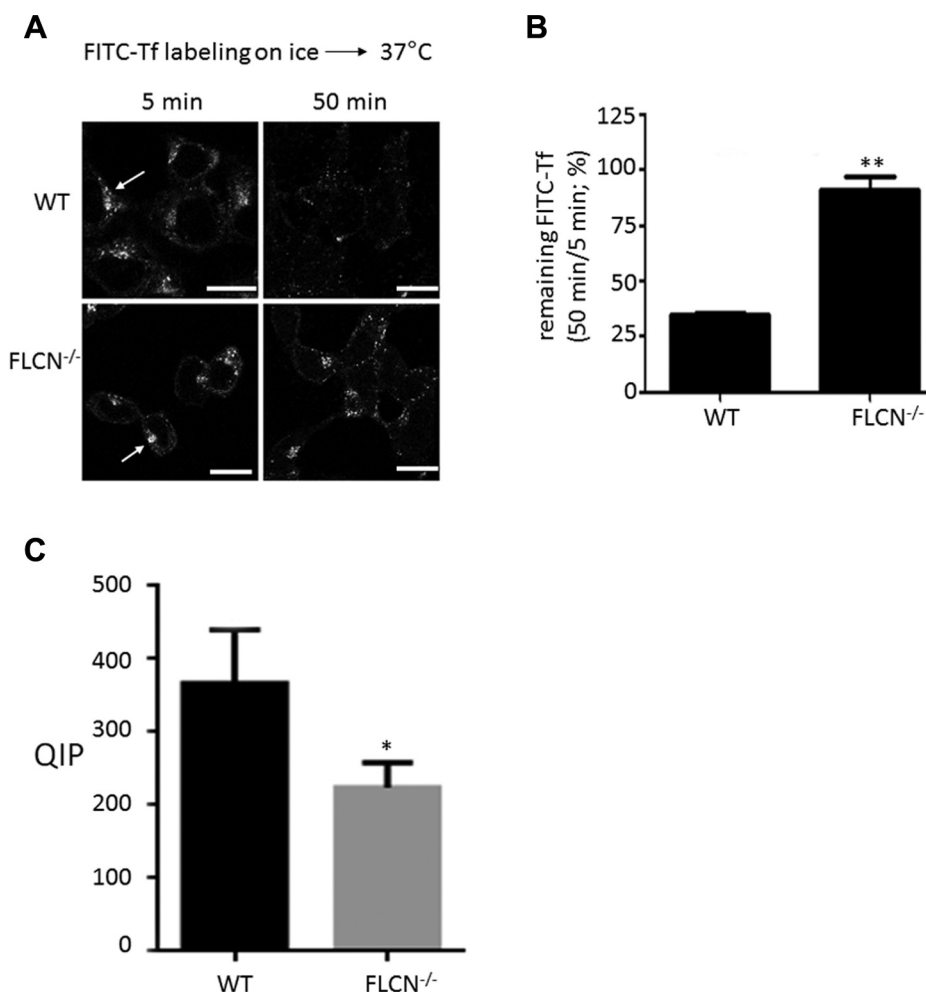


Figure 2. FLCN regulates the recycling transport of TfR1 and the uptake of Tf-iron. *A*, wild-type (WT) and *FLCN*^{-/-} cells were labeled with FITC-Tf, and confocal images are displayed. The *arrows* indicate the putative PRC sites at which Rab11A normally accumulates. Scale bars: 20 μ m. *B*, the intensity of the FITC-Tf signal as shown in *A* was measured with Nikon confocal software. At least 30 cells from each panel were evaluated. *C*, cells were stained with calcein-AM and were then incubated with holo-Tf for 3 h. Calcein fluorescence was measured by flow cytometry. Uptake of Tf-iron was indicated by the QIP (Δ MFI). MFI, median fluorescence intensity. * $p < 0.05$; ** $p < 0.01$.

found that the expression of both TfR1 and DMT1 was increased in several types of FLCN-deficient cells (49–51), including the patient-derived kidney tumor cell line UOK257 (Fig. 3F). We suspect that FLCN may regulate iron levels in a wide range of cell types.

In a previous study, we demonstrated that overexpression of FLCN promoted PAT1 recycling and amino acid absorption (9, 25). If FLCN regulates TfR1 transport in a similar dose-sensitive manner, increasing FLCN expression should accelerate TfR1 transport and iron uptake. Indeed, the expression of both TfR1 and DMT1 was decreased in three different FLCN-overexpressing cell lines, suggesting that these cells have high iron levels (Fig. 3G).

FLCN and Rab11A cooperatively regulate iron uptake

The current evidence suggests that FLCN promotes iron uptake through the Rab11A-mediated pathway. According to this model, depletion of Rab11A should inhibit iron uptake. Consistent with this hypothesis, both TfR1 and DMT1 were upregulated by Rab11A knockdown (Fig. 4A). In addition, this

effect was reversed by the addition of ferric ammonium citrate (FAC), a commonly used iron supplement (Fig. 4A).

Similar to other Rab GTPases, Rab11A is switched between an active GTP-bound and an inactive GDP-bound state. Overexpression of an active mutant of Rab11A (Q70L, Rab11A-act) counteracted FLCN knockdown by decreasing the expression of both TfR1 and DMT1 (Fig. 4B). This result, combined with the finding that FLCN physically interacts with Rab11A (Fig. 1), indicates that these two proteins probably cooperate to regulate iron uptake.

Increased HIF activity in *FLCN*^{-/-} cells is induced by low iron stress

FLCN can regulate many signaling pathways. Which of these pathways is responsive to the low iron status caused by FLCN loss? To address this question, we examined the expression of FLCN downstream genes in five different pathways: the cell adhesion (CDH1) (51), TGF- β (TGFB2 and INHBA) (51), PGC-1 α (PGC-1 α and PDK4) (10), TFE3/TFEB (GPNMB) (52), and HIF (BNIP3, VEGFA, and G6PD1) pathways (53).

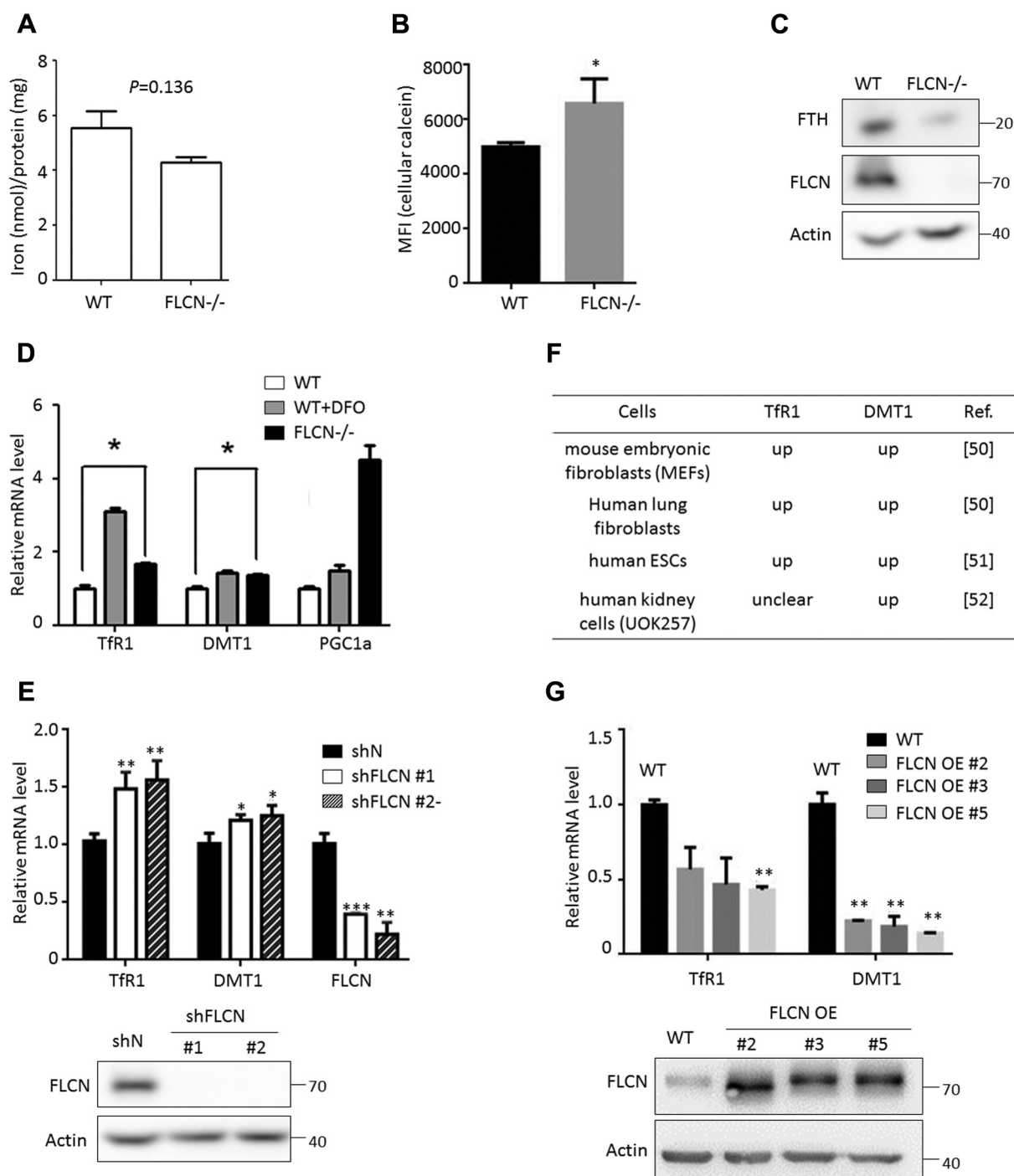


Figure 3. FLCN regulates the cellular iron pool. *A*, ferrozine assay of the total cellular iron concentration (*n* = 3 repeated experiments). *B*, assay of the labile iron pool by calcein-AM staining. Calcein fluorescence was measured by flow cytometry. FMI, median fluorescence intensity. *C*, WB showing that FTH expression was decreased by FLCN loss. *D*, *E*, and *G*; RT-PCR analysis of mRNA levels. In *E*, shN indicates the nonsense shRNA (negative control). In *G*, FLCN OE indicates FLCN overexpression. *F*, a brief summary of the published data showing the expression of TfR1 and DMT1 in different types of FLCN-deficient cells. **p* < 0.05; ***p* < 0.01; ****p* < 0.001.

The activity of three pathways, including PGC-1 α , TFEB/TFE3, and HIF, was changed in the same direction (increased) in both *FLCN*^{-/-} cells and wild-type cells deprived of iron (Fig. 5A). We then focused on these three pathways. We speculated that if the low iron pool is a main signal for activation of these pathways, increasing the iron supply (+FAC) should reverse these results. Indeed, the addition of FAC to

FLCN^{-/-} cells had little influence on the PGC-1 α expression (Fig. 5B) and the TFEB activity (Fig. 5C), indicating that decreased iron pool is not the major activator of PGC-1 α and TFEB in *FLCN*^{-/-} cells (Fig. 5A, and see Fig. 3D).

In contrast, the increased HIF activity in *FLCN*^{-/-} cells was reversed by FAC to a level similar to that in control cells (Fig. 5D). Moreover, iron deficiency (+DFO) induced HIF

FLCN regulates iron metabolism

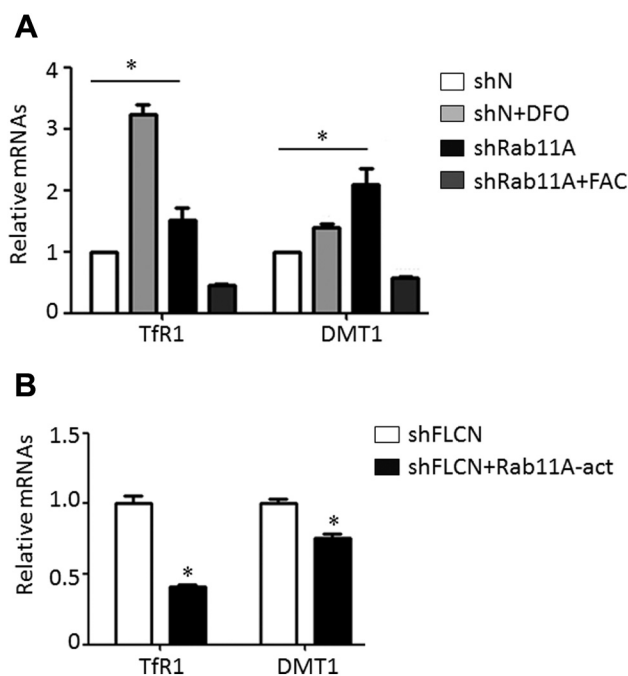


Figure 4. FLCN and Rab11A cooperatively regulate iron homeostasis (RT-PCR analysis). A, Rab11A knockdown (shRab11A) increased the expression of both TfR1 and DMT1, and this effect was reversed by FAC supplementation. B, increasing Rab11A activity by Rab11A-act expression counteracted the effect of FLCN knockdown. The stable cell lines of shFLCN (9) and shRab11A (25), and the Rab11A-act plasmid (active form of Rab11A) (25) have been described before.

activity more strongly than FLCN loss (Fig. 5A), and HIF activity in *FLCN*^{-/-} cells was further increased by DFO chelation (Fig. 5E). Taken together, these results strongly suggest that the increased HIF activity in *FLCN*^{-/-} cells was due mainly to low iron stress.

FLCN regulates iron metabolism in *Drosophila*

Previously, we constructed a *Drosophila* model of BHD syndrome by genetic deletion of the *FLCN* homolog, *DBHD* (26). Homozygous *DBHD* mutants (*DBHD*^{-/-}) could hatch from eggs, but the hatched larvae grew slowly and eventually died with small and thin bodies.

To explore whether iron metabolism is disrupted by *DBHD* deletion, we tried to rescue *DBHD* mutant larvae by feeding iron-rich food (normal food supplemented with FAC). FAC supplementation had no apparent toxicity in *DBHD* heterozygotes (+/-) because after supplementation with different doses of FAC, they could develop into healthy adults with no abnormalities in either development time (~10 days from eggs to adults) or body size. Interestingly, a small but considerable number of *DBHD* mutant larvae fed the FAC-supplemented diet developed into pupae, although the development time was prolonged (up to 3 weeks). Moreover, the rescued mutants could complete metamorphosis without noticeable developmental defects (Fig. 6A), but they could not eclose and eventually died as pharate pupae.

Another interesting observation is that the rescue efficiency seemed to be sensitive to the FAC dose. For example, at

0.4 mM FAC, approximately 43% of *DBHD*^{-/-} larvae developed into pupae; however, this percentage decreased when the FAC dose was either too low or too high (Fig. 6B). Because excess iron is toxic, we believe that the mutants may have defects in shutting down iron uptake systems and/or expelling excess iron from their bodies. Taken together, these results demonstrate that *DBHD* regulates iron metabolism in *Drosophila*.

Discussion

Our data reveal TfR1 as a new substrate transported by FLCN. An important finding is that TfR1 can physically interact with both Rab11A and FLCN, particularly under low-iron conditions (Fig. 1B). This result not only supports a role for FLCN in iron metabolism but also suggests that accelerating TfR1 transport might be an adaptive mechanism to promote iron uptake. FLCN preferentially binds with TfR1 *via* its N-terminal region, which contains a longin domain (LD). Because LDs have been found in several proteins involved in the membrane docking/fusion process, the last step of vesicular trafficking (54), FLCN is probably a scaffold protein mediating the interactions between Rabs and other transport machinery components.

Consistent with the role of FLCN during the Rab11A–TfR1 interaction, loss of FLCN delayed the recycling of TfR1, while the internalization of TfR1 from the cell surface was unaffected. These results are very similar to those of Rab11A suppression (55, 56). However, FLCN is unlikely to be a ubiquitous Rab11A-binding protein, because *Rab11A*^{-/-} mice died earlier than *FLCN*^{-/-} mice during embryonic stages due to the abolition of matrix metalloproteinase secretion upon Rab11A loss (55). We suspect that FLCN is one of the Rab11A-interacting proteins that determines cargo specificity.

Although our data were obtained mainly in HEK293 cells, FLCN may also regulate iron homeostasis in other cell types. By searching published databases, we found that both TfR1 and DMT1 were upregulated in several different types of FLCN-deficient cells from both humans and mice (Fig. 3F). However, other cell and animal models are needed to confirm whether regulation of iron homeostasis is a general function of FLCN. Using a *Drosophila* model of BHD syndrome, we demonstrated that loss of *DBHD* disrupted iron homeostasis in fruit flies. First, the *DBHD* mutants suffered from low-iron stress, which was relieved by feeding iron-rich food (Fig. 6A). Second, the mutants were intolerant to high levels of iron (Fig. 6B), probably because they could not eliminate the toxic iron. We previously showed that amino acids can rescue the development of most *DBHD* mutants into early pupae, albeit with failure to undergo metamorphosis (26). Compared with amino acids, iron rescued the development of only a small portion of *DBHD*^{-/-} larvae into pupae, and the duration of this developmental phase was prolonged. However, mutants rescued by iron supplementation could complete metamorphosis. These results suggest that amino acids and iron play different but partially redundant roles during *Drosophila* development. Amino acids contribute mainly to growth

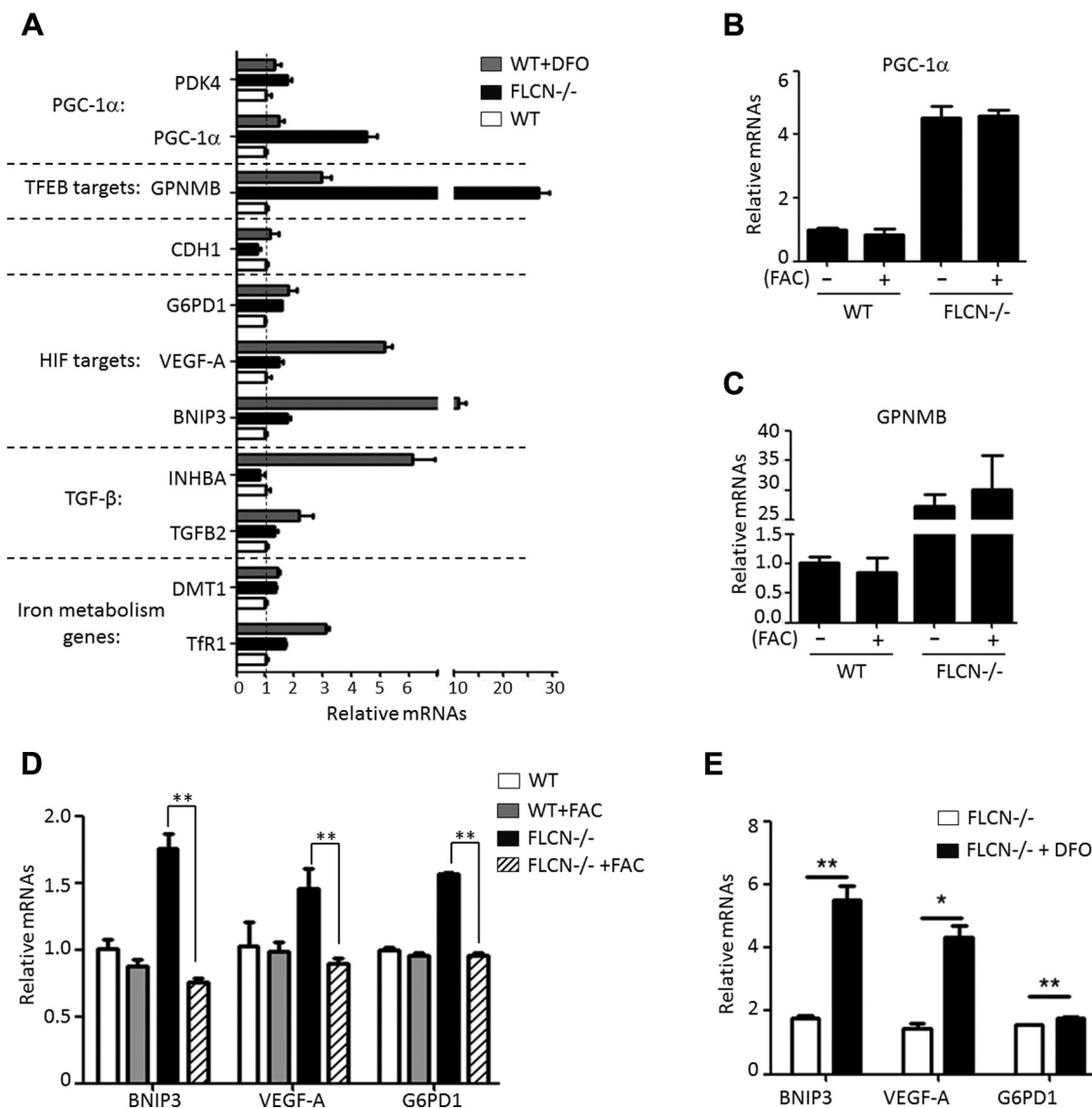


Figure 5. The increase in HIF activity upon FLCN loss is due to the iron deficiency condition (RT-PCR analysis). A, the activity of PGC-1α, TFEB, and HIFs was increased under both iron depletion (DFO chelation) and FLCN loss (FLCN^{-/-}) conditions. Note that DFO chelation increased the expression of both iron metabolism genes (TfR1 and DMT1) and HIF target genes more strongly than FLCN deficiency. B and C, iron supplementation (30 μM FAC for 4 h) had no effect on PGC-1α expression (B) or TFEB (C) activity in FLCN^{-/-} cells. D, The increase in HIF activity in FLCN^{-/-} cells was reversed by FAC supplementation. E, HIF activity in FLCN^{-/-} cells was increased further by DFO chelation.

(increasing cell number and size). This role is consistent with the classical amino-acid-activated mTOR pathway. In contrast, iron is indispensable for morphogenesis, and this role cannot be substituted by amino acids. Notably, iron also plays a role in growth, as supported by the following findings. First, iron rescued the development of a small portion of *DBHD*^{-/-} larvae into pupae with almost normal body sizes. Second, a previous study showed that iron can stimulate the proliferation of cultured *Drosophila* cells (57).

Our finding that FLCN regulates iron metabolism is consistent with the prediction that FLCN regulates fundamental biological processes. In fact, some of the FLCN^{-/-} phenotypes might be related to aberrant iron homeostasis. For example, blood cells are highly sensitive to the iron supply. Deletion of FLCN in mouse bone marrow exhausted the

population of hematopoietic stem/progenitor cells and depleted all hematopoietic cell lineages (58). In another study, loss of FNIP1 killed mouse B lymphocytes (59). An interesting question arises as to whether these hematopoietic phenotypes are caused by iron insufficiency. In addition, iron is important for the health of the tissues most commonly affected in BHD syndrome, including the skin, lung, and kidney. The skin is an organ that affects the systematic iron level; iron can be lost by sweat and desquamation of epidermal cells. The level of iron in the skin is variable and is associated with wound healing and skin aging. Both iron deficiency and iron overload can damage skin and skin appendages (60). The lung is constantly exposed to environmental stimuli, including various pathogens and iron-containing compounds. Iron metabolism in the lung must be tightly controlled to alleviate the oxidative stress caused by

FLCN regulates iron metabolism

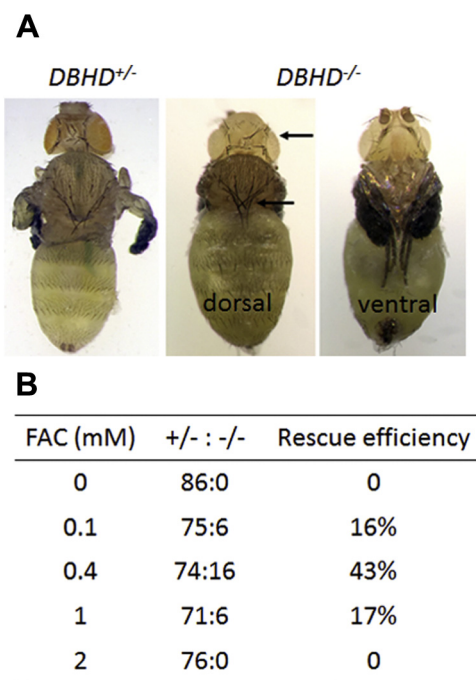


Figure 6. **A**, representative images of two male *Drosophila* pupae collected from the same tube of food supplemented with FAC. The mutant (*DBHD*^{-/-}) can be distinguished from the heterozygote (+/-) by the white eyes and long bristles (arrows). Note that the mutant has completed metamorphosis. **B**, quantification of the adults (+/-) and the rescued mutant pupae (-/-) from the same food tubes. The rescue efficiency was calculated as the ratio of the number of *DBHD*^{-/-} pupae to 1/2 the number of (+/-) adults. Note that high concentrations of FAC (>0.4 mM) were toxic to the mutants.

active immune and detoxification reactions (61). The kidney has been found to play important roles in the reabsorption of renal iron. Disruption of this process can result in systematic iron loss, which in turn impairs kidney function (62).

Iron is a critical nutrient for cell proliferation, and it is generally acknowledged that the iron level is increased in tumor cells because of their high demand for iron. However, there are some reports showing that the iron level is decreased in certain tumors (63, 64). Alternatively, the iron level in tumors may be variable, depending on the tumor stage and type. It is known that iron negatively regulates HIF. PHDs, which require iron as a cofactor, can modify key proline residues in the HIF protein, leading to recruitment of the tumor suppressor VHL and degradation of HIF through the ubiquitin-dependent proteasome pathway. In the absence of iron, PHDs are inactive, and HIF is stabilized (33). Loss of FLCN has been shown to activate HIF by increasing the ROS level (53). Here, we provide evidence that iron-deficient conditions are probably a major signal for HIF activation in *FLCN*^{-/-} cells. First, DFO chelation decreased the iron level and activated HIF more strongly than FLCN loss (Fig. 3A). Because the iron level was only slightly decreased in *FLCN*^{-/-} cells, HIF protein expression may not have been markedly induced (53). Second, the increased HIF activity in *FLCN*^{-/-} cells was reversed to the level in wild-type cells by iron supplementation (Fig. 3D). We propose that targeting iron metabolism to cure BHD lesions with increased HIF activity deserves further investigation.

Experimental procedures

Reagents

Antibodies specific for the following proteins were used: FLCN (Cell Signaling Technology; #3697), Tfr1 (Santa Cruz; #3B82A1), HA (Abcam; #9110), GFP (TransGen Biotech; #HT801), beta-actin (Sungene Biotech; #KM9001T), and Rab11A (BD Biosciences; #610656).

FITC-conjugated ChromPure Human Transferrin was purchased from Jackson ImmunoResearch Laboratories (; #009-090-050). DFO was purchased from Santa Cruz Biotechnology (#sc203331). Ferrozine (S30675) and neocuproine (#S30420) were purchased from YuanYe Bio-Technology. Propidium iodide (PI, #ST511) and a Cell Counting Kit-8 (#C0037) were purchased from Beyotime Biotechnology.

Cell culture

HEK293 cells were normally cultured in the following complete media: Dulbecco's modified Eagle's medium (DMEM) supplemented with 8% fetal bovine serum (FBS), 4 mM L-glutamine, 4500 mg/l glucose, sodium pyruvate; or RPMI 1640 medium (US Biological, R8999-04A). The cDNAs encoding FLCN variants tagged with HA were cloned into the pcDNA3.1(+) vector. The resulting plasmids were transfected into cells using TurboFect transfection reagent (Life Technology).

For the gene knockdown experiments, shRNA for either shFLCN or shRab11A was cloned into the pCD513B-U6 vector and cotransfected with the helper plasmids (GAG, REV, and VSV-G) into HEK293 cells. Lentiviruses containing the shRNAs were isolated and used to infect cells. Cells with stable gene knockdown were selected with puromycin. The shRNA target sequences were selected based on previous reports and included the following: shFLCN (9), TCAGTATGCAGTCG-CAATAAC and CTCTCAGCAAGTACGAGTTTG; Rab11A (25), GTAACCTCCTGTCTCGATTTAC and GGAGTAGAGTTTGCAACAAGA. For DFO or FAC treatment, the culture medium was replaced with complete DMEM containing 100 μ M DFO or 30 μ M FAC and incubated for different periods of time.

Co-IP and WB analysis

The co-IP assays were carried out essentially as described previously (9, 25). In some experiments, the cells were pre-treated with 100 μ M DFO before lysis.

FITC-Tf tracing assay

Cells were seeded on clean 13 mm square cover slides in 24-well plates. When the cells were ~80% confluent, the medium was replaced with serum-free RPMI 1640 medium for 45 min to exhaust the cellular Tf. The cell plate was cooled on ice for several minutes. Then, the medium was replaced with cold serum-free 1640 medium containing 20 μ g/ml FITC-Tf. Twenty minutes later, the medium was removed, and the cells were quickly washed twice with cold PBS and then for

2 min with a cold acid solution (500 mM NaCl, 0.2 N acetic acid (pH 2)) to block the FITC-Tf/TfR1 interaction. Cells were washed with cold complete medium for 5 min to restore the pH to neutral. Then, the cells were cultured in complete DMEM and transferred to 37 °C to reinstate endocytosis. At different time points, cells were fixed with 4% paraformaldehyde for 20 min at room temperature, washed with PBS, and imaged using a Nikon A1R confocal microscope. At least 30 cells from three repeated experiments in each assay were analyzed by one-way ANOVA followed by Fisher's least significant difference test using SPSS software (20.0, SPSS, Inc).

Colorimetric ferrozine assay

The total cellular iron concentration was measured using a ferrozine-based iron assay as described previously (65). Cells plated in 60 mm dishes (~80% confluence) were washed twice with cold PBS and lysed with 200 µl of 50 mM NaOH at -20 °C (or on ice) for 2 h. One-hundred microliters of cell lysate was mixed with 100 µl of HCl (100 mM) and 100 µl of fresh iron release solution (1.4 M HCl and 4.5% KMnO₄ in H₂O) and incubated at 60 °C for 2 h. After cooling to room temperature, 30 µl of iron detection reagent (6.5 mM ferrozine, 6.5 mM neocuproine, 2.5 M ammonium acetate, and 1 M ascorbic acid dissolved in H₂O) was added to each tube. After 30 min, 280 µl of the reaction solution was transferred into a well of a 96-well plate, and the absorbance was measured at 570 nm in a Bio-Rad Model 680 microplate reader. A standard curve was generated using FeCl₃ (0–100 µM) solutions. The iron concentration was normalized to the total protein concentration in the sample (as measured by the bicinchoninic acid method).

Calcein-AM staining and flow cytometric analysis

Cells were cultured in 6-well plates to ~80% confluence. Then, the culture medium was replaced with iron-free RPMI 1640 medium, and the cells were cultured for 40 min to deplete serum Tf. Then, the cells were stained with 0.4 µM calcein-AM (Beyotime Biotechnology, #C2012) at room temperature for 10 min. After several washes with warm PBS, the cells were incubated in RPMI 1640 medium with or without 10 µg/ml holo-Tf (Sigma-Aldrich Corp, #T0655) for 3 h.

The calcein-AM fluorescence signal in single cells was measured by flow cytometry in a BD FACSAria III system (~490 nm excitation and ~510 nm emission). For each sample, approximately 1 × 10⁴ cells were measured, and the data were analyzed using FlowJo Software. The QIP (ΔMFI) was calculated as follows: MFI (without holo-Tf chasing)-MFI (with holo-Tf chasing), where MFI is the median fluorescence intensity. The MFI value without holo-Tf chasing was also used to indicate the labile iron pool.

RT-PCR

Total cellular RNA was isolated using TRIzol reagent. One microgram of total RNA was used to synthesize first-strand cDNA using the Evo M-MLV system (Accurate Biotechnology; #ag11705). Real-time quantitative PCR (qPCR) was

performed based on SYBR Green detection (ABI) in a Bio-Rad CFX Connect system. The sequences of the primers used for RT-PCR are provided in the [Supplementary File](#).

Drosophila experiments

The *DBHD* knockout stock (*w; DBHD*⁻/*TM3, Sb, Kr-GFP*) was assayed (26). Because TM3 chromosome homozygosity is lethal, only heterozygotes (+/-) can survive to adulthood, and heterozygotes were thus used as the control in this study. Heterozygous (+/-) flies have red eyes, GFP expression, and abnormal bristles (*Sb*), by which they can be easily distinguished from their mutant (-/-) siblings. Flies were maintained at 25 °C with 60% humidity. The fly food generally used in our laboratory contains 8% sugar, 10% corn flour, 1.5% baker's yeast, 1% agar, 0.4% propionic acid, and 0.1% Nipagin. To prepare the FAC food, the food vials were heated in a microwave oven, and FAC was added into the melted food to the indicated concentrations. Embryos were collected every ~12 h by transferring the parent flies into a new food vial. The rescue efficiency was calculated as the ratio of the number of *DBHD*^{-/-} pupae to 1/2 the number of (+/-) adults.

Data availability

All data are contained in the text.

Supporting information—This article contains [supporting information](#) (9, 51, 52).

Author contributions—W. L. conceived the study, designed the experiments. X. W., H. W., and L. Z. performed the experiments. Z. L. and M. Q. provided help in some experiments. Y. J. provided the reagents. X. W., H. W., L. Z., and W. L. analyzed the data. W. L. wrote the article.

Funding and additional information—This work was supported by the National Natural Science Foundation of China (31372256) to W. L. and was partly supported by Program of Shaanxi Province Science and Technology Innovation Team (2019TD-036).

Conflict of interest—The authors declare that they have no conflicts of interest with the contents of this article.

Abbreviations—The abbreviations used are: BHD, Birt-Hogg-Dubé; co-IP, coimmunoprecipitation; DENN, differentially expressed in normal cells and neoplasia; DMEM, Dulbecco's modified Eagle's medium; DMT1, divalent metal transporter 1; FITC-Tf, fluorescence conjugated transferrin; FLCN, folliculin; GAP, GTPase-activating protein; HIF, hypoxia-inducible factor; HRE, hypoxia response element; IRE, iron-responsive element; PHD, prolyl hydroxylase; PRC, perinuclear recycling center; QIP, quenched iron pool; TfR1, transferrin receptor 1; WB, western blot.

References

- Nickerson, M. L., Warren, M. B., Toro, J. R., Matrosova, V., Glenn, G., Turner, M. L., Duray, P., Merino, M., Choyke, P., Pavlovich, C. P., Sharma, N., Walther, M., Munroe, D., Hill, R., Maher, E., *et al.* (2002)

- Mutations in a novel gene lead to kidney tumors, lung wall defects, and benign tumors of the hair follicle in patients with the Birt-Hogg-Dubé syndrome. *Cancer Cell* **2**, 157–164
2. Baba, M., Furihata, M., Hong, S. B., Tessarollo, L., Haines, D. C., Southon, E., Patel, V., Igarashi, P., Alvord, W. G., Leighty, R., Yao, M., Bernardo, M., Ileva, L., Choyke, P., Warren, M. B., *et al.* (2008) Kidney-targeted Birt-Hogg-Dubé, gene inactivation in a mouse model: Erk1/2 and Akt-mTOR activation, cell hyperproliferation, and polycystic kidneys. *J. Natl. Cancer Inst.* **100**, 140–154
 3. Chen, J., Futami, K., Petillo, D., Peng, J., Wang, P., Knol, J., Li, Y., Khoo, S. K., Huang, D., Qian, C. N., Zhao, P., Dykema, K., Zhang, R., Cao, B., Yang, X. J., *et al.* (2008) Deficiency of FLCN in mouse kidney led to development of polycystic kidneys and renal neoplasia. *PLoS One* **3**, e3581
 4. Wu, M., Si, S., Li, Y., Schoen, S., Xiao, G. Q., Li, X., Teh, B. T., Wu, G., and Chen, J. (2015) Flcn-deficient renal cells are tumorigenic and sensitive to mTOR suppression. *Oncotarget* **6**, 32761–32773
 5. Gijzen, L. M., Vernooij, M., Martens, H., Oduber, C. E., Henquet, C. J., Starink, T. M., Prins, M. H., Menko, F. H., Nelemans, P. J., and van Steensel, M. A. (2014) Topical rapamycin as a treatment for fibrofolliculomas in Birt-Hogg-Dubé syndrome: A double-blind placebo-controlled randomized split-face trial. *PLoS One* **9**, e99071
 6. Hartman, T. R., Nicolas, E., Klein-Szanto, A., Al-Saleem, T., Cash, T. P., Simon, M. C., and Henske, E. P. (2009b) The role of the Birt-Hogg-Dubé protein in mTOR activation and renal tumorigenesis. *Oncogene* **28**, 1594–1604
 7. Petit, C. S., Rocznik-Ferguson, A., and Ferguson, S. M. (2013) Recruitment of folliculin to lysosomes supports the amino acid-dependent activation of Rag GTPases. *J. Cell Biol.* **202**, 1107–1122
 8. Tsun, Z. Y., Bar-Peled, L., Chantranupong, L., Zoncu, R., Wang, T., Kim, C., Spooner, E., and Sabatini, D. M. (2013) The folliculin tumor suppressor is a GAP for the RagC/D GTPases that signal amino acid levels to mTORC1. *Mol. Cell* **52**, 495–505
 9. Wu, X., Zhao, L., Chen, Z., Ji, X., Qiao, X., Jin, Y., and Liu, W. (2016) FLCN maintains the leucine level in lysosome to stimulate mTORC1. *PLoS One* **11**, e0157100
 10. Yan, M., Gingras, M. C., Dunlop, E. A., Nouët, Y., Dupuy, F., Jalali, Z., Possik, E., Coull, B. J., Kharitidi, D., Dydensborg, A. B., Faubert, B., Kamps, M., Sabourin, S., Preston, R. S., Davies, D. M., *et al.* (2014) The tumor suppressor folliculin regulates AMPK-dependent metabolic transformation. *J. Clin. Invest.* **124**, 2640–2650
 11. Possik, E., Jalali, Z., Nouët, Y., Yan, M., Gingras, M. C., Schmeisser, K., Panaite, L., Dupuy, F., Kharitidi, D., Chotard, L., Jones, R. G., Hall, D. H., and Pause, A. (2014) Folliculin regulates ampk-dependent autophagy and metabolic stress survival. *PLoS Genet.* **10**, e1004273
 12. Yan, M., Audet-Walsh, É., Manteghi, S., Dufour, C. R., Walker, B., Baba, M., St-Pierre, J., Giguère, V., and Pause, A. (2016) Chronic AMPK activation via loss of FLCN induces functional beige adipose tissue through PGC-1 α /ERR α . *Genes Dev.* **30**, 1034–1046
 13. Hasumi, Y., Baba, M., Hasumi, H., Huang, Y., Lang, M., Reindorf, R., Oh, H. B., Sciarretta, S., Nagashima, K., Haines, D. C., Schneider, M. D., Adelstein, R. S., Schmidt, L. S., Sadoshima, J., and Linehan, M. W. (2014) Folliculin (Flcn) inactivation leads to murine cardiac hypertrophy through mTORC1 deregulation. *Hum. Mol. Genet.* **23**, 5706–5719
 14. Roberg, K. J., Bickel, S., Rowley, N., and Kaiser, C. A. (1997) Control of amino-acid permease sorting in the late secretory pathway of *Saccharomyces cerevisiae* by SEC13, LST4, LST7, and LST8. *Genetics* **147**, 1569–1584
 15. van Slegtenhorst, M., Khabibullin, D., Hartman, T. R., Nicolas, E., Kruger, W. D., and Henske, E. P. (2007) The Birt-Hogg-Dubé and tuberous sclerosis complex homologs have opposing roles in amino acid homeostasis in *Schizosaccharomyces pombe*. *J. Biol. Chem.* **282**, 24583–24590
 16. Péli-Gulli, M.-P., Sardu, A., Panchaud, N., Raucci, S., and De Virgilio, C. (2015) Amino acids stimulate TORC1 through Lst4-Lst7, a GTPase-activating protein complex for the Rag family GTPase Gtr2. *Cell Rep.* **13**, 1–7
 17. Pacitto, A., Ascher, D. B., Wong, L. H., Blaszczyk, B. K., Nookala, R. K., Zhang, N., Dokudovskaya, S., Levine, T. P., and Blundell, T. L. (2015) Lst4, the yeast Fni1/2 orthologue, is a DENN-family protein. *Open Biol.* **5**, 150174
 18. Baba, M., Hong, S. B., Sharma, N., Warren, M. B., Nickerson, M. L., Iwamatsu, A., Esposito, D., Gillette, W. K., Hopkins 3rd, R. F., Hartley, J. L., Furihata, M., Oishi, S., Zhen, W., Burke Jr, T. R., Linehan, W. M., *et al.* (2006) Folliculin encoded by the BHD gene interacts with a binding protein, FNIP1, and AMPK, and is involved in AMPK and mTOR signaling. *Proc. Natl. Acad. Sci. U. S. A.* **103**, 15552–15557
 19. Hasumi, H., Baba, M., Hong, S. B., Hasumi, Y., Huang, Y., Yao, M., Valera, V. A., Linehan, W. M., and Schmidt, L. S. (2008) Identification and characterization of a novel folliculin-interacting protein FNIP2. *Gene* **415**, 60–67
 20. Takagi, Y., Kobayashi, T., Shiono, M., Wang, L., Piao, X., Sun, G., Zhang, D., Abe, M., Hagiwara, Y., Takahashi, K., and Hino, O. (2008) Interaction of folliculin (Birt-Hogg-Dubé gene product) with a novel Fni1-like (Fni1L/Fni2) protein. *Oncogene* **27**, 5339–5347
 21. Hasumi, H., Baba, M., Hasumi, Y., Lang, M., Huang, Y., Oh, H. F., Matsuo, H., Merino, M. J., Yao, M., Ito, Y., Furuya, M., Iribe, Y., Kodama, T., Southon, E., Tessarollo, L., *et al.* (2015) Folliculin-interacting proteins Fni1 and Fni2 play critical roles in kidney tumor suppression in cooperation with Flcn. *Proc. Natl. Acad. Sci. U. S. A.* **112**, E1624–E1631
 22. Nookala, R. K., Langemeyer, L., Pacitto, A., Ochoa-Montaño, B., Donaldson, J. C., Blaszczyk, B. K., Chirgadze, D. Y., Barr, F. A., Bazan, J. F., and Blundell, T. L. (2012) Crystal structure of folliculin reveals a hidden DENN function in genetically inherited renal cancer. *Open Biol.* **2**, 120071
 23. Zheng, J., Duan, B., Sun, S., Cui, J., Du, J., and Zhang, Y. (2017) Folliculin interacts with Rab35 to regulate EGF-induced EGFR degradation. *Front. Pharmacol.* **8**, 688
 24. Laviolette, L. A., Mermoud, J., Calvo, I. A., Olson, N., Boukhali, M., Steinlein, O. K., Roeder, E., Sattler, E. C., Huang, D., Teh, B. T., Motamedi, M., Haas, W., and Iliopoulos, O. (2017) Negative regulation of EGFR signalling by the human folliculin tumour suppressor protein. *Nat. Commun.* **8**, 15866
 25. Zhao, L., Ji, X., Zhang, X., Li, L., Jin, Y., and Liu, W. (2018) FLCN is a novel Rab11A-interacting protein that is involved in the Rab11A-mediated recycling transport. *J. Cell Sci.* **131**, jcs218792
 26. Liu, W., Chen, Z., Ma, Y., Wu, X., Jin, Y., and Hou, S. (2013) Genetic characterization of the *Drosophila* Birt-Hogg-Dubé syndrome gene. *PLoS One* **8**, e65869
 27. Starling, G. P., Yip, Y. Y., Sanger, A., Morton, P. E., Eden, E. R., and Dodding, M. P. (2016) Folliculin directs the formation of a Rab34–RILP complex to control the nutrient-dependent dynamic distribution of lysosomes. *EMBO Rep.* **17**, e201541382–e201541841
 28. Muckenthaler, M. U., Rivella, S., Hentze, M. W., and Galy, B. (2017) A red carpet for iron metabolism. *Cell* **168**, 344–361
 29. Lim, J. E., Jin, O., Bennett, C., Morgan, K., Wang, F., Trenor 3rd, C. C., Fleming, M. D., and Andrews, N. C. (2005) A mutation in Sec15l1 causes anemia in hemoglobin deficit (hbd) mice. *Nat. Genet.* **37**, 1270–1273
 30. Chen, C., Garcia-Santos, D., Ishikawa, Y., Seguin, A., Li, L., Fegan, K. H., Hildick-Smith, G. J., Shah, D. I., Cooney, J. D., Chen, W., King, M. J., Yien, Y. Y., Schultz, I. J., Anderson, H., Dalton, A. J., *et al.* (2013) Snx3 regulates recycling of the transferrin receptor and iron assimilation. *Cell Metab.* **17**, 343–352
 31. Kawabata, H. (2019) Transferrin and transferrin receptors update. *Free Radic. Biol. Med.* **133**, 46–54
 32. Bianchi, L., Tacchini, L., and Cairo, G. (1999) HIF-1-mediated activation of transferrin receptor gene transcription by iron chelation. *Nucleic Acids Res.* **27**, 4223–4227
 33. Wang, G. L., and Semenza, G. L. (1993) Desferrioxamine induces erythropoietin gene expression and hypoxia-inducible factor 1 DNA-binding activity: Implications for models of hypoxia signal transduction. *Blood* **82**, 3610–3615
 34. Owen, D., and Kühn, L. C. (1987) Noncoding 3' sequences of the transferrin receptor gene are required for mRNA regulation by iron. *EMBO J.* **6**, 1287–1293
 35. Anderson, C. P., Shen, M., and Eisenstein, R. S. (2012) Leibold EA Mammalian iron metabolism and its control by iron regulatory proteins. *Biochim. Biophys. Acta* **1823**, 1468–1483

36. Kühn, L. C. (2015) Iron regulatory proteins and their role in controlling iron metabolism. *Metallomics* **7**, 232–243
37. Matsui, T., Itoh, T., and Fukuda, M. (2011) Small GTPase Rab12 regulates constitutive degradation of transferrin receptor. *Traffic* **12**, 1432–1443
38. Raiborg, C., Bache, K. G., Gillooly, D. J., Madshus, I. H., Stang, E., and Stenmark, H. (2002) Hrs sorts ubiquitinated proteins into clathrin-coated microdomains of early endosomes. *Nat. Cell Biol.* **4**, 394–398
39. Fujita, H., Iwabu, Y., Tokunaga, K., and Tanaka, Y. (2013) Membrane-associated RING-CH (MARCH) 8 mediates the ubiquitination and lysosomal degradation of the transferrin receptor. *J. Cell Sci.* **126**, 2798–2809
40. Tong, X., Kawabata, H., and Koeffler, H. P. (2002) Iron deficiency can upregulate expression of transferrin receptor at both the mRNA and protein level. *Br. J. Haematol.* **116**, 458–464
41. Chaston, T. B., and Richardson, D. R. (2003) Iron chelators for the treatment of iron overload disease: Relationship between structure, redox activity, and toxicity. *Am. J. Hematol.* **73**, 200–210
42. Grant, B. D., and Donaldson, J. G. (2009) Pathways and mechanisms of endocytic recycling. *Nat. Rev. Mol. Cell Biol.* **10**, 597–608
43. Stenmark, H. (2009) Rab GTPases as coordinators of vesicle traffic. *Nat. Rev. Mol. Cell Biol.* **10**, 513–525
44. Riedelberger, M., and Kuchler, K. (2020) Analyzing the quenchable iron pool in murine macrophages by flow cytometry. *Bio-protocol* **10**, e3552
45. Wang, D., Wang, L. H., Zhao, Y., Lu, Y. P., and Zhu, L. (2010) Hypoxia regulates the ferrous iron uptake and reactive oxygen species level via divalent metal transporter 1 (DMT1) Exon1B by hypoxia-inducible factor-1. *IUBMB Life* **62**, 629–636
46. Klomp, J. A., Petillo, D., Niemi, N. M., Dykema, K. J., Chen, J., Yang, X. J., Säaf, A., Zickert, P., Aly, M., Bergerheim, U., Nordenskjöld, M., Gad, S., Giraud, S., Denoux, Y., Yonneau, L., *et al.* (2010) Birt-Hogg-Dubé renal tumors are genetically distinct from other renal neoplasias and are associated with up-regulation of mitochondrial gene expression. *BMC Med. Genomics* **3**, 59
47. Hasumi, H., Baba, M., Hasumi, Y., Huang, Y., Oh, H. F., Hughes, R. M., Klein, M. E., Takikita, S., Nagashima, K., Schmidt, L. S., and Linehan, W. M. (2012) Regulation of mitochondrial oxidative metabolism by tumor suppressor FLCN. *J. Natl. Cancer Inst.* **104**, 1750–1764
48. Wada, S., Neinast, M., Jang, C., Ibrahim, Y. H., Lee, G., Babu, A., Li, J., Hoshino, A., Rowe, G. C., Rhee, J., Martina, J. A., Puertollano, R., Blenis, J., Morley, M., Baur, J. A., *et al.* (2016) The tumor suppressor FLCN mediates an alternate mTOR pathway to regulate browning of adipose tissue. *Genes Dev.* **30**, 2551–2564
49. Kennedy, J. C., Khabibullin, D., Hougard, T., Nijmeh, J., Shi, W., and Henske, E. P. (2019) Loss of FLCN inhibits canonical WNT signaling via TFE3. *Hum. Mol. Genet.* **28**, 3270–3281
50. Mathieu, J., Detraux, D., Kuppers, D., Wang, Y., Cavanaugh, C., Sidhu, S., Levy, S., Robitaille, A. M., Ferreccio, A., Bortorff, T., McAlister, A., Somasundaram, L., Artoni, F., Battle, S., Hawkins, R. D., *et al.* (2019) Folliculin regulates mTORC1/2 and WNT pathways in early human pluripotency. *Nat. Commun.* **10**, 632
51. Hong, S. B., Oh, H., Valera, V. A., Stull, J., Ngo, D. T., Baba, M., Merino, M. J., Linehan, W. M., and Schmidt, L. S. (2010) Tumor suppressor FLCN inhibits tumorigenesis of a FLCN-null renal cancer cell line and regulates expression of key molecules in TGF-beta signaling. *Mol. Cancer* **9**, 160
52. Hong, S. B., Oh, H., Valera, V. A., Baba, M., Schmidt, L. S., and Linehan, W. M. (2010) Inactivation of the FLCN tumor suppressor gene induces TFE3 transcriptional activity by increasing its nuclear localization. *PLoS One* **5**, e15793
53. Preston, R. S., Philp, A., Claessens, T., Gijzen, L., Dydensborg, A. B., Dunlop, E. A., Harper, K. T., Brinkhuizen, T., Menko, F. H., Davies, D. M., Land, S. C., Pause, A., Baar, K., van Steensel, M. A., and Tee, A. R. (2010) Absence of the Birt-Hogg-Dubé gene product is associated with increased hypoxia-inducible factor transcriptional activity and a loss of metabolic flexibility. *Oncogene* **30**, 1159–1173
54. Rossi, V., Banfield, D. K., Vacca, M., Dietrich, L. E., Ungermann, C., D'Esposito, M., Galli, T., and Filippini, F. (2004) Longins and their longin domains: Regulated SNAREs and multifunctional SNARE regulators. *Trends Biochem. Sci.* **29**, 682–688
55. Yu, S., Yehia, G., Wang, J., Stypulkowski, E., Sakamori, R., Jiang, P., Hernandez-Enriquez, B., Tran, T. S., Bonder, E. M., Guo, W., and Gao, N. (2014) Global ablation of mouse rab11a impairs early embryogenesis and matrix metalloproteinase secretion. *J. Biol. Chem.* **289**, 32030–32043
56. Ullrich, O., Reinsch, S., Urbé, S., Zerial, M., and Parton, R. (1996) Rab11 regulates recycling through the pericentriolar recycling endosome. *J. Cell Biol.* **135**, 913–924
57. Li, S. (2010) Identification of iron-loaded ferritin as an essential mitogen for cell proliferation and postembryonic development in *Drosophila*. *Cell Res.* **20**, 1148–1157
58. Baba, M., Toyama, H., Sun, L., Takubo, K., Suh, H. C., Hasumi, H., Nakamura-Ishizu, A., Hasumi, Y., Klarmann, K. D., Nakagata, N., Schmidt, L. S., Linehan, W. M., Suda, T., and Keller, J. R. (2016) Loss of Folliculin disrupts hematopoietic stem cell quiescence and homeostasis resulting in bone marrow failure. *Stem Cells* **34**, 1068–1082
59. Baba, M., Keller, J. R., Sun, H. W., Resch, W., Kuchen, S., Suh, H. C., Hasumi, H., Hasumi, Y., Kieffer-Kwon, K. R., Gonzalez, C. G., Hughes, R. M., Klein, M. E., Oh, H. F., Bible, P., and Southon, E. (2012) The folliculin-FNIP1 pathway deleted in human Birt-Hogg-Dubé syndrome is required for murine B-cell development. *Blood* **120**, 1254–1261
60. Wright, J. A., Richards, T., and Srai, S. K. S. (2014) The role of iron in the skin and cutaneous wound healing. *Front. Pharmacol.* **5**, 156
61. Ghio, A. J. (2009) Disruption of iron homeostasis and lung disease. *Biochim. Biophys. Acta* **1790**, 731–739
62. van Swelm, R. P. L., Wetzels, J. F. M., and Swinkels, D. W. (2020) The multifaceted role of iron in renal health and disease. *Nat. Rev. Nephrol.* **16**, 77–98
63. Cui, C., Cheng, X., Yan, L., Ding, H., Guan, X., Zhang, W., Tian, X., and Hao, C. (2019) Downregulation of Tfr1 promotes progression of colorectal cancer via the JAK/STAT pathway. *Cancer Manag. Res.* **11**, 6323–6341
64. Greene, C. J., Attwood, K., Sharma, N. J., Gross, K. W., Smith, G. J., Xu, B., and Kauffman, E. C. (2017) Transferrin receptor 1 upregulation in primary tumor and downregulation in benign kidney is associated with progression and mortality in renal cell carcinoma patients. *Oncotarget* **8**, 107052–107075
65. Barbeito, A. G., Levade, T., Delisle, M. B., Ghetti, B., and Vidal, R. (2010) Abnormal iron metabolism in fibroblasts from a patient with the neurodegenerative disease hereditary ferritinopathy. *Mol. Neurodegener.* **5**, 50